Pergamon

Cement and Concrete Research, Vol. 25, No. 5, pp. 989–998, 1995
Copyright © 1995 Elsevier Science Ltd
Printed in the USA. All rights reserved
0008-8846/95 $9.50 + .00

0008-8846(95)00094-1

INFLUENCE OF CATHODE-TO-ANODE AREA RATIO AND SEPARATION DISTANCE ON GALVANIC CORROSION CURRENTS OF STEEL IN CONCRETE CONTAINING CHLORIDES

C. Arya
School of Architecture and Civil Engineering
South Bank University
Wandsworth Road, London SW8 2JZ.

P.R.W Vassie
Transport Research Laboratory
Concrete Bridges Division
Old Wokingham Road
Crowthorne, Berkshire RG11 6AU.

(Refereed)
(Received August 19, 1994; in final form April 12, 1995)

ABSTRACT

Corrosion of steel embedded in concrete was modelled using a 4m long beam containing a bar in seven segments, one mild steel and six stainless steel, which could be electrically connected or isolated by external switches. The concrete mix was dosed with 3% Cl to initiate corrosion. The current flowing between the mild steel and the stainless steel was monitored using a zero resistance ammeter for a range of connections to investigate the influence of the ratio of cathode/anode area and cathode-anode separation.

It was found that the current increased with increasing cathode/anode area ratio but the rate of increase decreased with increasing cathode/anode ratio. The current decreased with increasing separation between the anode and cathode although the cathode elements most distant from the anode contributed a significant current.

Introduction

The deterioration of concrete structures, primarily as a result of reinforcement corrosion, is a world wide problem [1]. The main cause of reinforcement corrosion is identified as the presence of chlorides in concrete [2]. The chlorides mainly originate from external sources such as sea-water and de-icing salts. The chlorides destroy the protective oxide film which develops on the steel surface as a result of the highly alkaline conditions found in quality concrete and in the presence of oxygen and moisture allow corrosion to occur [3].

Several approaches have been suggested for combating this problem, the most practical being to delay the onset of corrosion either by increasing the depth of concrete cover of the reinforcing bars, silane treatments [4] and/or specifying cement extenders such as PFA [5] and GGBS [6] to reduce concrete

permeability. However, these measures have proved to have limited success in delaying the time to corrosion. In order to prevent reinforcement corrosion during the life of structures steps also need to be taken to reduce the rate of corrosion following initiation.

Macrocell corrosion is known to produce pitting of reinforcing steel in concrete structures resulting in substantial reductions in the cross sectional area of the reinforcing bars and sometimes severance of the bar [7]. Macrocell corrosion can occur when the concrete contains chlorides and has a high moisture content. These conditions increase the electrical conductivity of the concrete allowing higher currents to pass and the effective cathode area to increase. Half cell potential surveys on structures have shown that the potential of steel reinforcement at distances in excess of a metre from the anodic site is polarised [8]. This polarisation indicates that steel more than a metre from the anodic site is acting as a cathode and is contributing current to the macrocell. This paper makes a preliminary investigation of some factors that may affect the magnitude of the corrosion current with a view to finding practical ways to limit macrocell currents and the corrosion damage that they cause in concrete structures. The effect of the cathode area and the distance between the anode and cathode sites on the galvanic current are the main factors investigated using a simple uni-dimensional cell.

Although it is straightforward to measure the potential of the steel in different parts of a macrocell using either embedded or external reference cells it has proved much more difficult to interpret macrocell current measurements. Three techniques have been used by investigators to measure macrocell currents; they are linear polarisation resistance, direct measure of galvanic current and electrochemical noise.

It has been shown that steel undergoing pitting or crevice corrosion has a distinctive noise signature allowing these forms of corrosion to be detected at an early stage [9,10]. If noise techniques could be effectively quantified the currents produced would provide a good guide to the rate of corrosion.

Linear polarisation resistance is an established method for measuring corrosion currents. However, in order to convert the corrosion current into a corrosion rate with units of loss in bar diameter per unit time, it is also necessary to know the area of the anode. It is possible to control the length of steel bar that receives the potential perturbation using a guard ring [11] but it is not usually possible to assess what proportion of this bar length is acting as an anode. The other techniques would also have this limitation. There are conflicting reports in the literature concerning the effectiveness of the linear polarisation resistance method for measuring corrosion currents of macrocells particularly when some cathodic areas are distant from the anode. Slater [12] reports considerable reservations concerning the use of linear polarisation resistance for measuring macrocell corrosion rates whereas Andrade [13] has had some success using a mathematical model based on transmission lines.

The direct measurement of galvanic current has been used effectively by some investigators [14,15,16]. It has the advantage that the current measured is that naturally flowing and does not result from any perturbation of the system. Its main disadvantage is that currents flowing within either of the two electrodes are not included and thus the measured galvanic current may be less than the true corrosion current [17]. For some systems this effect can be significant, notably when the resistance of the concrete is too high to support the macrocell activity. In this case the galvanic current could be zero whereas there is sufficient microcell activity to produce a significant rate of corrosion.

In the present study it was decided to measure galvanic currents because the simplicity of instrumentation and data interpretation was appropriate for a preliminary investigation. Furthermore our objective of investigating the effect of anode-cathode separation and our specimen design indicated that galvanic current measurement was the best approach. In order to minimise the influence of microcell activity the area of the mild steel electrode, the nominal anode within our cell, was kept to a minimum.

Test Parameters

The main factors influencing the galvanic current which have been examined in this study are the ratio of cathode to anode area [14] and the distance between the cathode and anode. A brief investigation of the following variables was also made:

1. Concrete quality
2. Relative humidity
3. Temperature
4. Electrical resistance of the concrete.

Experimental details

To carry out this study a model of a linear corroding reinforcing bar was used as shown in Figure 1 [15]. The system was made up of six segments of AISI type 316 stainless steel reinforcement, 25 mm in diameter and 600-665 mm in length. The ends of the segments were tapped and connected to adjacent sections using short lengths of threaded nylon rod. The nylon also served to insulate adjacent sections of reinforcement. The centre bar of the assembly was a segment of mild steel reinforcement, 25 mm in diameter and 20 mm in length. The length of this segment was kept short in order to restrict the area of cathodic region within the mild steel. Each segment was electrically connected at one point using stainless steel type 316 wire, sleeved with PTFE. This was to allow any or all of the stainless steel segments to be electrically connected to the mild steel section via an external connection.

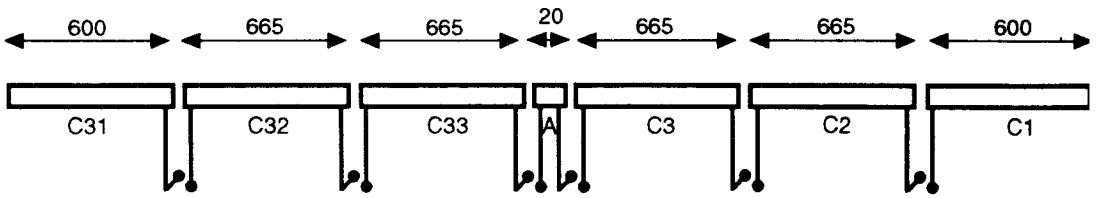

A - Anode, Mild Steel
C1, C2, C3, C31, C32, C33 - Cathodes, Stainless Steel
Dimensions in mm

FIG. 1
Layout of segmented bar with all switches in the open circuit position

The segmented bar was placed centrally in a steel mould, 80 mm by 155 mm by 4000 mm long. Silver-silver chloride, half-cells (P_O, P1, P2, P31, P32) were attached to the segmented bar at the positions shown on Figure 2 using nylon ties. Prior to concreting, the stainless steel segments and the ends of the half cells were coated in a polymer modified cementitious grout in order to achieve good bond with the concrete.

Two beams were cast. The mixes proportions used are given in Table 1. The chloride content in both mixes was 3% by weight of cement. The chloride ions were introduced by dissolving appropriate quantities of sodium chloride into the mix water.

Resistance probes (R_O, R3, R31), each consisting of four stainless steel (type 316) plates of dimensions, 10mm x 10mm, and stainless steel connecting wire (Fig. 3) were cast into the beams at the locations shown in Figure 2.

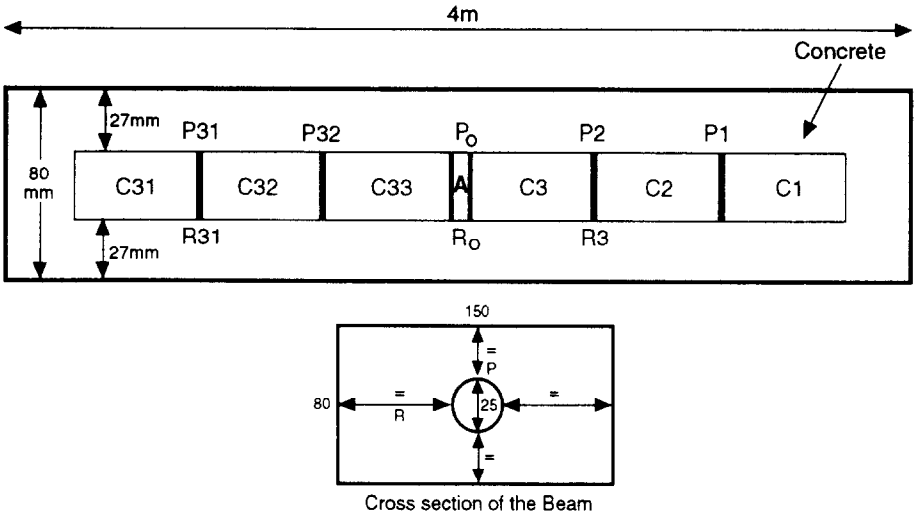

FIG. 2
The Test Beam showing the position of anodes, cathodes, reference electrodes and resistance probes.

The beams were cured for 56 days in a fog room at a relative humidity of 95% and temperature of 21°C prior to testing.

The galvanic currents flowing in the beam for various anode-cathode combinations were measured using an ACM zero resistance ammeter. The resistances between the centre poles of the probes were measured using an AC bridge to give a measure of the concrete resistances at the three probe sites. In all cases, the galvanic currents and half cell potentials were measured once steady state conditions were attained.

TABLE 1
Mix proportions

	Beam A	Beam B
OPC	1	1
Zone 2 Sand	2.4	1.5
Thames Valley Flint 10mm	2.9	3
Water	0.65	0.45
Superplasticiser	_	1.7%
NaCl	3% Cl*	3% Cl*

* by weight of cement

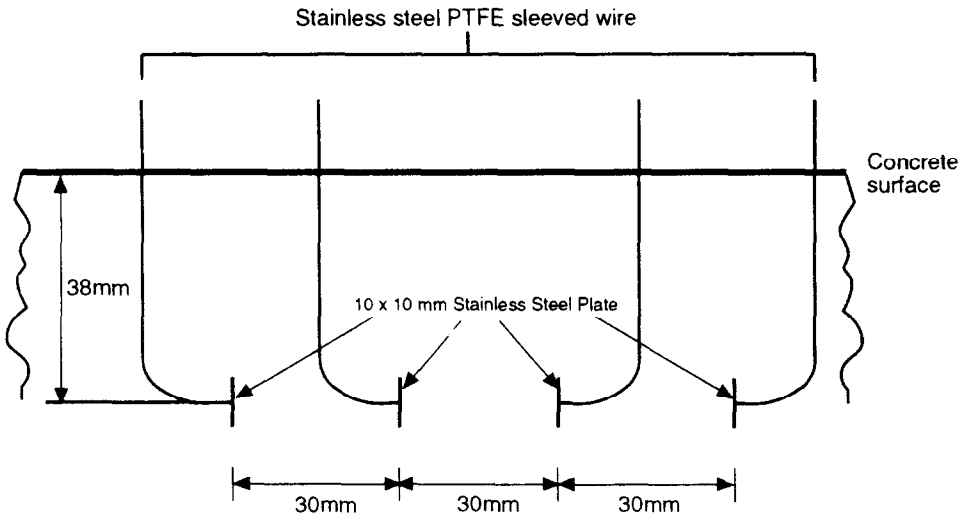

FIG. 3
Resistance probes

Results and Discussion

(1) Concrete compressive strength and resistivity

Table 2 shows the average 28 day compressive strengths for the concretes used in beams A and B. Table 3 shows the average resistances in beams A and B.

The resistances of the two mixes were quite similar. This was probably attributable to the high concentration of chlorides present in both mixes and the high moisture content of the concretes due to the 95% relative humidity conditions under which the beams were stored.

TABLE 2
Average 28 day compressive strengths

	Beam A	Beam B
Compressive strength (N/mm^2)	31	44

TABLE 3
Average resistances in beams A and B

Resistance Probe	Resistance (Ohms)	
	Beam A	Beam B
R31	200	250
R_o	215	260
R3	190	250

(2) Cathode/anode ratio

Fig. 4 shows the steady-state current densities in beams A and B as a function of cathode/anode area ratio. The current density is the galvanic current divided by the area of the mild steel segment. In both cases the stainless steel segments (cathodes) were electrically connected to the mild steel (anode) in the order C3,C33,C2,C32,C1,C31.

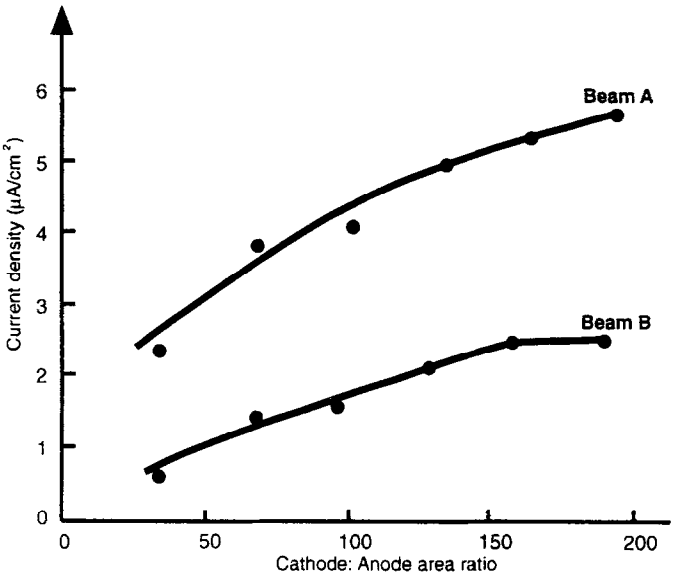

FIG. 4
Effect of cathode to anode area ratio on the current density

The current density of both beams increased significantly as the cathode/anode area ratio increased i.e. as more lengths of stainless steel were connected to the anode, due to an increase in the cathodic surface random reactions. The rate of increase in current density decreased as the cathode/anode ratio increased. This is probably due to ohmic polarisation as the anode-cathode separation increases. Limitations resulting from the rate at which ferrous ions can be transported away from the anode may also contribute to this effect.

The current densities were considerably higher in beam A than beam B, presumably due to the fact that the concrete in beam B had a lower water/cement ratio and hence lower permeability than in beam A. The lower current obtained from the low permeability mix can probably be explained by:

1) the higher resistances measured in beam B, even though both beams contained 3% Cl by weight of cement

2) lower rates of transport of oxygen and ferrous ions producing restrictions to the cathode and anode reaction kinetics.

(3) Distance between anode and cathode

Table 4 shows the steady-state current densities in beams A and B due to various (mild steel) anode to (stainless steel) cathode connections.

TABLE 4
Effect of distance to anode on current density

Anode to cathode connection	Current density (μA/cm^2)	
	Beam A	Beam B
A-C1	1.53	0.32
A-C2	1.91	0.22
A-C3	2.36	0.64
A-C1-C31	2.80	0.57
A-C2-C32	3.50	0.54
A-C3-C33	3.85	1.37

It can be seen that, generally, for a given cathode/anode ratio, the greater the distance between the anode and cathode, the smaller the current density. Moreover, with the better quality mix in beam B, the reduction in current density with distance is more pronounced.

The only effect of increasing the anode-cathode separation is to increase the length of the return path for negative ions transferring charge from the cathode to the anode through the concrete. This ohmic effect substantially reduces the current although it is worth noting that even the most distant cathode contributes significantly to the corrosion current.

The development of a concrete mix that limits the throwing power of the anode would produce a marked reduction in the area of the cathode and hence also in the corrosion current in concrete structures. The test beam used in this study had the reinforcement in one dimension only whereas in a structure reinforcement cages are three dimensional, therefore a reduction in the throwing power of the spheroidal anode field in a structure would result in a much greater reduction in cathode area than was achieved in the test beams.

(4) Anode and cathode potentials

Figure 5 for beams A and B plot the half-cell potentials with respect to the nearest embedded Ag/AgCl reference cell for each section of the reinforcing bar when all the sections are connected together.

Tables 5 and 6, for beams A and B respectively, compare the potentials of each section in the connected and isolated modes. These results clearly show that even cathode sections more than a metre distant from the anode are being significantly polarised. For example, there is a 200mV difference between the isolated and connected potentials for cathode C1 in beam B which suggests that the anode-cathode distance would have to be several metres before the isolated and connected potentials became equal, indicating that the steel at such a distance from the anode was unpolarised. However comparing Tables 4 to 6 shows that there is little correspondence between the amount of polarisation and the current contributed by equivalent cathode sections in beams A and B.

The large throwing power of anodes in beams A and B explains why large reductions in bar cross-section can occur over very short time spans in concrete structures and perhaps suggests that one way of avoiding this problem would be to electrically isolate bars in reinforcement cages.

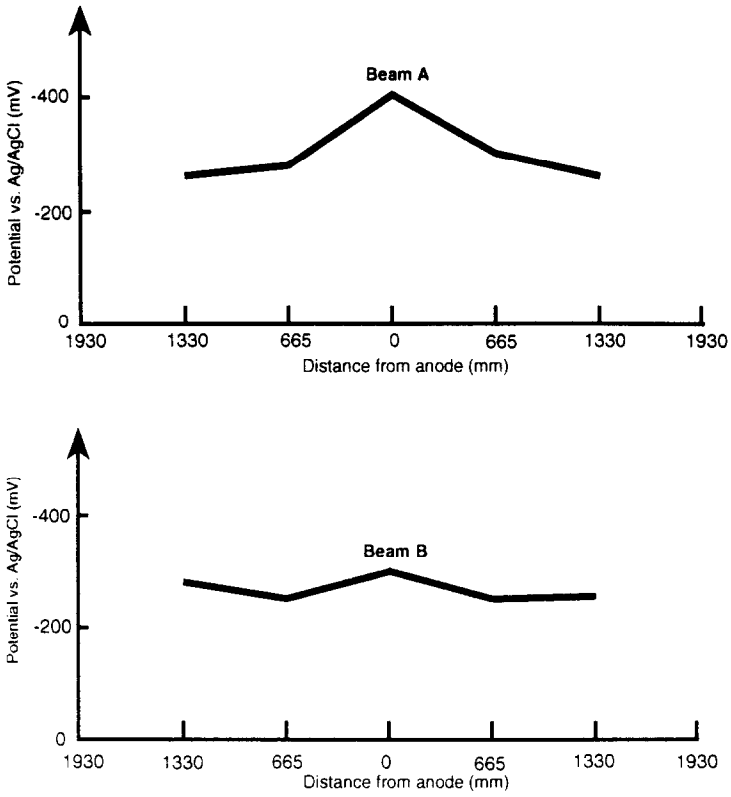

FIG. 5
Potential readings for Beams A and B with all the bars segments connected

(5) Effect of temperature and relative humidity

Table 7 shows the combined effects of relative humidity and temperature of the external storage environment on the steady-state current densities for beam A.

The intention was that the effect of both parameters should be independently assessed. However, in practice this was difficult to achieve. Nevertheless, the results showed that both factors have a

TABLE 5
Potentials of cathode elements for Beam A in the isolated and connected modes, versus the Ag/AgCl reference electrodes

Cathode	Potential (mV)	
	Isolated	Connected
C31	-35	-260
C32	-30	-300
C33	-70	-370
C1	-40	-270
C2	-50	-320
C3	-100	-360

TABLE 6
Potentials of cathode elements for Beam B in the isolated and connected modes, versus the Ag/AgCl reference electrodes

Cathode	Potential (mV)	
	Isolated	Connected
C31	-160	-280
C32	-120	-260
C33	-100	-340
C1	-100	-300
C2	-95	-270
C3	-85	-330

TABLE 7
Effect of temperature and relative humidity on current density

Anode to cathode connection	Temp (°C)	Relative humidity	Current density ($\mu A/cm^2$)
A-C1-C31	21	71%	1.34
A-C1-C31	21	95%	2.80
A-C1-C31	31	80%	3.18

significant effect on current density. Generally, the current density increased with increasing temperature and relative humidity.

Conclusions

1) The corrosion current increased with increasing cathode/anode area ratio up to a cathode/anode ratio of at least 190. However, the rate of increase decreased as the cathode/anode ratio increased.

2) The throwing power of the anode exceeded a distance of one metre although the current contributed by the cathode sections decreased with increasing anode-cathode separation.

3) The potentials of the most distant cathodes indicated that they were polarised by the anode, but the potential measurements of the cathodes did not provide a reliable measure of the amount of current they contributed.

4) The corrosion currents from the beam made from the better quality concrete were much lower than for the poor quality mix. Thus it is possible that the use of a very dense concrete may reduce the current to an insignificant level by minimising the throwing power of the anode. Dense concrete would also increase the time to corrosion by inhibiting transport processes.

Acknowledgements

The authors would like to thank Dr. Chris Naish of AERE Harwell for his helpful suggestions and advice and Mr John King of South Bank University for his technical assistance.

References

1. J. P. Broomfield, Proc. Instn. Civ. Engrs, Structs. and Bldgs.,104,211,May 1994.
2. E. J. Wallbank, The Performance of Concrete Bridges: A 200 Bridge Survey, Dept. of Transport, Her Majesties Stationery Office, London, 1989.
3. D. G. Manning, Concr. Int.,7,20,May 1985.
4. Department of Transport, Impregnation of Concrete Highway Structure, Department Advice Note BA33/90, Her Majesties Stationery Office, London, 1990.
5. P. Schiesl and R. Hardlt, Proc. P. K. Metha Symposium on Durability of Concrete, Nice, France,99,1994.
6. P. B. Bamforth and W. F. Price, Proc. Int. Conference: Concrete 2000, Univ. Dundee, Scotland, Ed. R. K. Dhir and M. R. Jones,2,1105,1993.
7. P. R. Vassie, Proc. Inst. Civ. Engrs. Part 1,76,713,1984.
8. P Cavalier & P Vassie, Proc. Instn. Civ. Engrs. Part 1, 70, 461 (1981).
9. K. Hladky and J. L. Dawson, Corrosion Science, 21, 317 (1981).
10. K. Hladky and J. L. Dawson, Corrosion Science, 22, 231 (1982).
11. C. Andrade et al, Proc. NACE Corrosion 92, Paper 194 (1992)
12. J. Slater. Corrosion of Metals In Association with Concrete, p40. ASTM STP818 (1983).
13. C. Andrade et al, Corrosion Rate of Steel in Concrete, ASTM STP 1065, N.S. Berke, V. Chaker and D. Whiting, Eds, 134 (1990).
14. K. Hollinshead and P. R. Vassie, Proc. Conference on U.K. Corrosion 89, Blackpool, 199, 1989.
15. C. C. Naish et al, Proc. Third Int. Symposium on Corrosion of Reinforcement in Concrete, U.K., Ed. C. L. Page et al, Elsevier, 1990.
16. P. Schiesl and M. Schwarzkopf, Betonwerk + Fertigteil-Technic, 10, 626 (1986).
17. N. S. Berke, D. F. Sherr and K. M. Sindberg, Corrosion Rates of Steel in Concrete. ASTM STP 1065, N.S. Berke, V. Chaker and D. Whiting, Eds, 38 (1990).